Gas-phase reactions of atomic lanthanide cations with methyl chloride - Perio...
Xiang Zhao; Gregory K Koyanagi; Diethard K Bohme
Canadian Journal of Chemistry; Nov 2005; 83, 11; Research Library
pg. 1839

Gas-phase reactions of atomic lanthanide cations with methyl chloride — Periodicities in reactivity[1]

Xiang Zhao, Gregory K. Koyanagi, and Diethard K. Bohme

Abstract: Room temperature reactions of lanthanide atomic cations (excluding Pm^+) with CH_3Cl are surveyed systematically in the gas phase using an inductively coupled plasma/selected-ion flow tube (ICP/SIFT) tandem mass spectrometer. Reaction rate coefficients are reported along with product distributions in He at 0.35 Torr (1 Torr = 133.3224 Pa) and 295 K. Cl atom transfer is the predominant reaction channel observed with all 14 lanthanide cations, but minor CH_3Cl addition also occurs with the late lanthanide cations Dy^+, Ho^+, Er^+, Tm^+, and Yb^+. The reaction efficiency for Cl atom transfer is shown to be governed by the energy required to promote an electron to achieve a d^1s^1 excited electronic configuration in which two non-f electrons are available for bonding: it decreases as the promotion energy increases and the periodic trend in reaction efficiency along the lanthanide series matches the periodic trend in the corresponding electron-promotion energy. This behaviour is consistent with a C—Cl bond insertion mechanism of the type proposed previously for insertion reactions of Ln^+ cations with hydrocarbons and methyl fluoride. Direct Cl atom abstraction by a harpoonlike mechanism was excluded because of an observed noncorrelation of reaction efficiency with $IE(Ln^+)$. A remarkable Arrhenius-like correlation is observed for the dependence of reactivity on promotion energy: the early and late lanthanide cations exhibit characteristic temperatures of $(1.4 \pm 0.2) \times 10^4$ and $(4.5 \pm 0.3) \times 10^3$ K, respectively. A rapid second Cl atom transfer occurs with $LaCl^+$, $CeCl^+$, $GdCl^+$, $TbCl^+$, and $LuCl^+$, but there was no evidence for a third chlorine atom abstraction with any of the $LnCl_2^+$ cations. Both $LnCl^+$ and $LnCl_2^+$ add up to five methyl chloride molecules under the experimental operating conditions of the ICP/SIFT tandem mass spectrometer.

Key words: lanthanide cations, Cl atom transfer, electron promotion, methyl chloride.

Résumé : Faisant appel à un spectromètre de masse en tandem avec plasma à couplage induit/tube d'écoulement d'ion choisi (« ICP/SIFT »), on a étudié d'une façon extensive les réactions en phase gazeuse et à la température ambiante du CH_3Cl avec les cations atomiques des lanthanides, à l'exception du Pm^+. On a mesuré les coefficients des vitesses réactionnelles ainsi que les distributions des produits dans He, à 0,35 Torr (1 Torr = 133,3224 Pa) et à 295 K. On a observé que le transfert d'un atome de chlore est la voie réactionnelle prédominante pour les quatorze cations de lanthanides, mais il se produit aussi une faible addition de CH_3Cl avec les derniers cations de lanthanides, Dy^+, Ho^+, Er^+, Tm^+ et Yb^+. On a démontré que l'efficacité de la réaction de transfert de l'atome de chlore est gouvernée par l'énergie requise pour faire passer un électron à la configuration électronique excitée d^1s^1 dans laquelle deux électrons non-f sont disponibles pour créer une liaison: elle diminue avec une augmentation de l'énergie nécessaire pour atteindre ce niveau et la tendance périodique observée dans l'efficacité de la réaction dans la série des lanthanides suit bien la tendance dans l'énergie correspondante nécessaire pour la promotion de l'électron. Ce comportement est en accord avec le type de mécanisme d'insertion dans une liaison C—Cl qui a été suggéré antérieurement pour les réactions d'insertion des cations de Ln^+ dans les hydrocarbures et le fluorure de méthyle. On a exclu un mécanisme de type harpon avec enlèvement direct d'un atome de chlore en raison du manque de corrélation qui a été observé pour la dépendance de la réactivité sur l'énergie de promotion: les cations du début et de la fin de la série des lanthanides des températures caractéristiques de $(1,4 \pm 0,2) \times 10^4$ et $(4,5 \pm 0,3) \times 10^3$ K, respectivement. Un deuxième transfert rapide d'un atome de chlore se produit avec le $LaCl^+$, le $CeCl^+$, le $GdCl^+$, le $TbCl^+$ et le $LuCl^+$, mais on n'a pas trouvé de données pouvant supporter un troisième transfert d'un atome de chlore à partir d'un cation quelconque de $LnCl_2^+$. Le $LnCl^+$ et le $LnCl_2^+$ ajoutent chacun jusqu'à cinq molécules de chlorure de méthyle dans les conditions expérimentales d'opération du spectromètre de masse en tandem ICP/SIFT.

Mots clés : cations de lanthanides, transfert d'atomes de chlore, promotion d'un électron, chlorure de méthyle.

[Traduit par la Rédaction]

Received 5 May 2005. Published on the NRC Research Press Web site at http://canjchem.nrc.ca on 16 December 2005.

X. Zhao, G.K. Koyanagi, and D.K. Bohme.[2] Department of Chemistry, Centre for Research in Mass Spectrometry and Centre for Research in Earth and Space Science, York University, Toronto, ON M3J 1P3, Canada.

[1] This article is part of a Special Issue dedicated to Professor P. Kebarle.

[2] Corresponding author (e-mail: dkbohme@yorku.ca).

doi: 10.1139/V05-198

Introduction

Recent laboratory measurements have shown that the unique electronic configurations of lanthanide cations lead to unique trends in the kinetics of chemical bond activation by these cations across the periodic table. As early as 1988, Shilling and Beauchamp (1) proposed that electron promotion from the $4f^n6s^1$ ground state to the $4f^{n-1}5d^16s^1$ excited state was required for these cations to be effective in C—H and C—C bond activation and insertion. A plethora of investigations into lanthanide ion chemistry followed, in part to further characterize this requirement, but also motivated by general interests in the gas-phase and solution chemistry of lanthanides (2). Reactions of Ln^+ cations now have been investigated systematically with various inorganic and organic molecules, including hydrogen (3), oxygen (4), nitrous oxide (4), alkanes and cycloalkanes, alkenes (1, 5, 6), alcohol (7–9), benzene and substituted benzenes (10, 11), phenol (12), orthoformates (10, 13), ferrocene, and iron pentacarbonyl (14). Generally these studies show that the reactivity of Ln^+ varies along the 4f series often in a manner that appears to be determined by the accessibility, through electron promotion, of excited electronic configurations of the Ln^+ cations with two unpaired non-f electrons. Results with N_2O (4), O_2 (4), and CH_3F (15) have also revealed intriguing Arrhenius-like dependencies of the reactivity of the Ln^+ cation on the electron promotion energy, which exhibit different characteristic temperatures for the early and late lanthanide cations.

Here we present a survey of gas-phase reactions of all the lanthanide cations (except Pm^+, which does not have a stable isotope) using inductively coupled plasma/selected-ion flow tube (ICP/SIFT) tandem mass spectrometry (4, 16, 17). The aim of this work is to expand on our previous studies of gas-phase reactions of lanthanide cations with CH_3F (15). We are not aware of any previous studies of reactions of atomic lanthanide cations with chlorinated hydrocarbons.

Experimental section

The experiments were performed with the ICP/SIFT tandem mass spectrometer that has been described in detail previously (4, 16, 17). The atomic ions were generated within an atmospheric pressure argon plasma at 5500 K fed with a vaporized solution containing the lanthanide salt. The ions emerging from the ICP were injected through a differentially pumped sampling interface into a quadrupole mass filter and after mass analysis, introduced through an aspiratorlike interface into flowing helium carrier gas at 0.35 Torr (1 Torr = 133.3224 Pa) and 295 ± 2 K. After experiencing about 10^5 collisions with He atoms, the ions were allowed to react with CH_3Cl added into the flow tube.

The lanthanide ions emerging from the plasma initially have a Boltzmann internal energy distribution characteristic of the plasma temperature. However, these emerging hot populations are expected to be downgraded during the approximately 20 ms duration before entry into the reaction region in the flow tube. Energy degradation can occur by radiative decay as well as by collisions with argon atoms and the 10^5 collisions with He before entry into the reaction region. The extent to which quenching of any electronically excited states of the lanthanide cations that may be formed within the ICP is complete is uncertain and could be inferred only indirectly from the observed decays of primary ion signals. The observed semilogarithmic decays of the reacting lanthanide cations were invariably linear, often over as much as four decades of ion depletion, and so were indicative of single-state populations. This was also the case in our earlier studies with methyl fluoride (15). The many collisions with Ar and He between the source and the reaction region should ensure that the atomic ions reach a translational temperature equal to the tube temperature of 295 ± 2 K prior to entering the reaction region.

Reactant and product ions were sampled at the end of the flow tube with a second quadrupole mass filter and were measured as a function of added reactant. The resulting profiles provide information about reaction rate coefficients and product–ion distributions. Rate coefficients for primary reactions were determined with an uncertainty estimated to be less than ±30% from the semilogarithmic decay of the reactant ion intensity as a function of added reactant.

Methyl chloride was introduced into the reaction region of the SIFT as a dilute mixture in helium (~10%). The methyl chloride was obtained commercially and was of high purity (Matheson Gas Products, Whitby, Ontario, 99.5%).

Results and discussion

The reactions of 14 lanthanide cations were investigated with CH_3Cl. Both the primary and higher order reactions were monitored. Results obtained for the reactions of La^+, Gd^+, Dy^+, and Lu^+ are shown in Fig. 1. Table 1 summarizes the measured rate coefficients, reaction efficiencies, and product distributions. The reaction efficiency is taken to be equal to the ratio k/k_c, where k is the experimentally measured rate coefficient and k_c is the capture or collision rate coefficient. k_c was computed using the algorithm of the modified variational transition-state/classical trajectory theory developed by Su and Chesnavich (18) with $\alpha(CH_3Cl) = 4.72 \times 10^{-24}$ cm³ (19) and $\mu_D(CH_3Cl) = 1.896$ D (19).

Only Cl atom transfer (rxn. [1*a*]) and adduct formation (rxn. [1*b*]) were observed as primary reaction channels.

$$[1a] \quad Ln^+ + CH_3Cl \rightarrow LnCl^+ + CH_3$$

$$[1b] \quad \rightarrow Ln^+(CH_3Cl)$$

Adduct formation is a minor channel (≤30%) and was observed to compete only with the late Ln^+ cations Dy^+, Ho^+, Er^+, Tm^+, and Yb^+. As expected from the much lower first ionization energy of the lanthanides (IE(Ln)), all <6.3 eV, than that for CH_3Cl (11.29 eV) (20), electron transfer was not observed with any of the Ln^+ cations. The C—H bond activation channel (rxn. [1*c*]) is not competitive because it is quite endothermic since $D(H\text{-}CH_2Cl) >> HA(Ln^+)$, the H-atom affinity of the atomic lanthanide ions. $D(H\text{-}CH_2Cl) = 100.2 \pm 0.6$ kcal mol⁻¹ (19), whereas, for example, $HA(La^+) = 57.1 \pm 2.8$ kcal mol⁻¹ and $HA(Lu^+) = 48.8 \pm 3.6$ kcal mol⁻¹ (21).

$$[1c] \quad Ln^+ + CH_3Cl \rightarrow LnH^+ + CH_2Cl$$

A fast ($k \geq 1.4 \times 10^{-10}$ cm³ molecule⁻¹ s⁻¹) second chlorine atom abstraction (rxn. [2]) was observed with $LaCl^+$ (25), $CeCl^+$ (28), $GdCl^+$ (16), $TbCl^+$ (14), $DyCl^+$ (1.4), $HoCl^+$ (2.3), and $LuCl^+$ (17), where the rate coefficient is

Fig. 1. Composite of ICP/SIFT results for the reactions of the lanthanide metal ions La^+, Gd^+, Dy^+, and Lu^+ with CH_3Cl in helium buffer gas at 0.35 ± 0.01 Torr (1 Torr = 133.3224 Pa) and 295 ± 2 K.

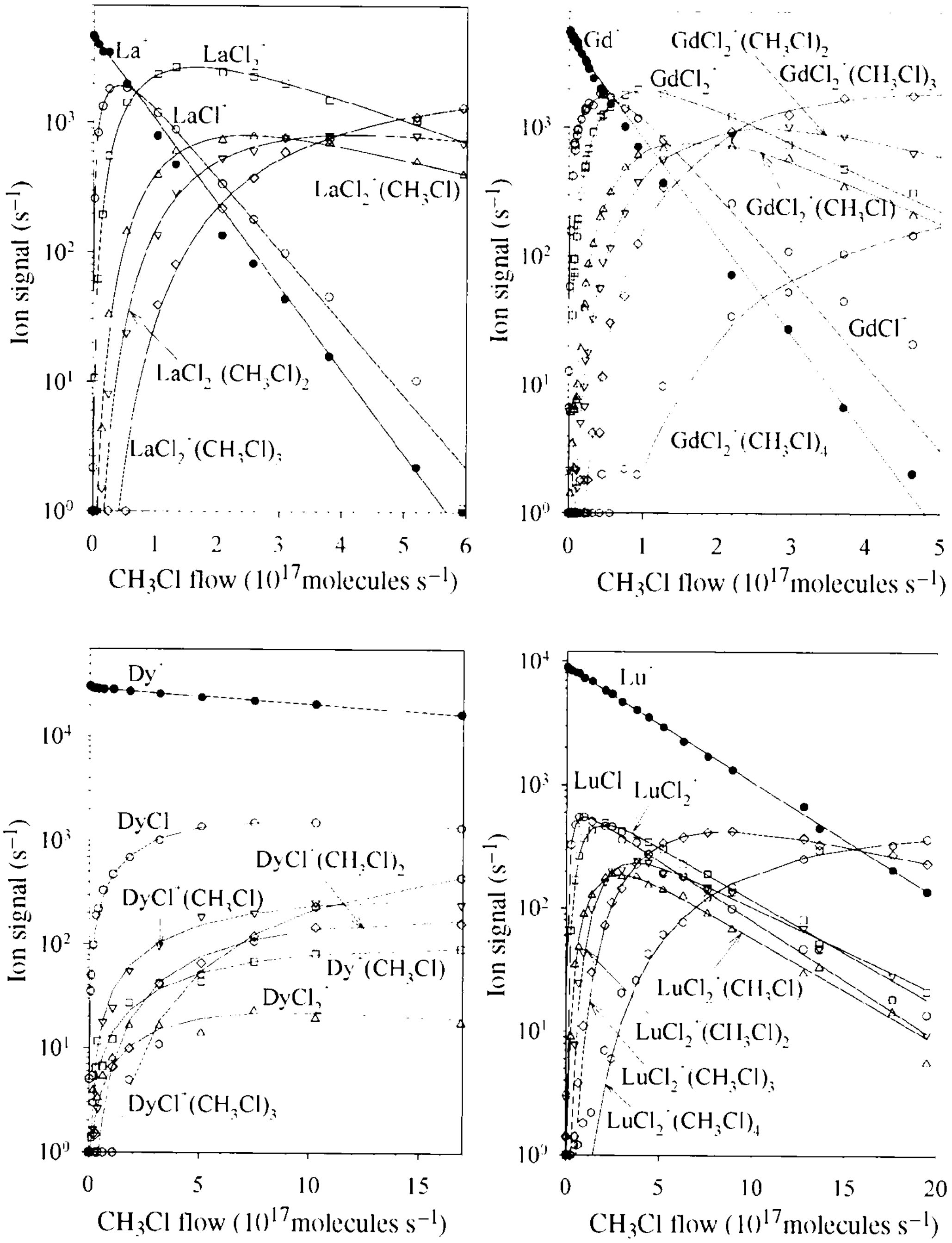

given in parentheses in units of 10^{-10} cm^3 $molecule^{-1}$ s^{-1}. These rate coefficients were obtained by curve fitting of the ion profiles for $LnCl^+$ and are less accurate than those for the primary reactions (the first few have values above k_c). The remaining $LnCl^+$ cations react with CH_3Cl with rate coefficients equal to or less than that measured for the first abstraction. No third Cl atom abstraction was observed with any of the $LnCl_2^+$ cations.

$$[2] \quad LnCl^+ + CH_3Cl \rightarrow LnCl_2^+ + CH_3$$

CH_3Cl addition according to rxn. [3] was also observed for almost all of the lanthanide chloride cations. These addition reactions are expected to be termolecular with He buffer – gas atoms acting as the stabilizing third body.

$$[3] \quad LnCl_m^+(CH_3Cl)_n + CH_3Cl \rightarrow LnCl_m^+(CH_3Cl)_{n+1} \quad (m = 0\text{–}2)$$

Secondary and higher order CH_3Cl addition was observed for $LnCl^+$ = $YbCl^+$ (m = 1, n = 0 to 1), $PrCl^+$, $DyCl^+$ (m = 1, n = 0–2), $NdCl^+$, $SmCl^+$, $EuCl^+$, $HoCl^+$ (m = 1, n = 0–3), $PrCl^+$ (m = 1, n = 1–4), and $LnCl_2^+$ = $LaCl_2^+$ (m = 2, n = 0–2), $CeCl^+$, $PrCl^+$, $GdCl_2^+$, $HoCl_2^+$, $LuCl_2^+$ (m = 2, n = 0–3). Table 1 includes a listing of all the higher order prod-

Table 1. First rate coefficients (in 10^{-10} cm^3 molecule^{-1} s^{-1}), reaction efficiencies (k/k_c), and higher order product ions measured for reactions of atomic cations Ln^+ with CH_3Cl in helium at 0.35 ± 0.01 Torr (1 Torr = 133.3224 Pa) and 295 ± 2 K.

M^+	k^a	k_c^b	k/k_c	Primary products	PD^c	Higher order product ions
La^+	11	17.2	0.62	$LaCl^+$	100	$LaCl_2^+$, $LaCl_2^+(CH_3Cl)_{1-3}$
Ce^+	9.5	17.2	0.55	$CeCl^+$	100	$CeCl_2^+$, $CeCl_2^+(CH_3Cl)_{1-4}$
Pr^+	2.3	17.2	0.13	$PrCl^+$	100	$PrCl_2^+$, $PrCl^+(CH_3Cl)_{1-5}$, $PrCl_2^+(CH_3Cl)_{1-4}$
Nd^+	1.9	17.2	0.11	$NdCl^+$	100	$NdCl^+(CH_3Cl)_{1-4}$
Sm^+	1.1	17.0	0.064	$SmCl^+$	100	$SmCl(CH_3Cl)_{1-4}$
Eu^+	0.33	17.0	0.019	$EuCl^+$	100	$EuCl^+(CH_3Cl)_{1-4}$
Gd^+	10	17.0	0.59	$GdCl^+$	100	$GdCl_2^+$, $GdCl_2^+(CH_3Cl)_{1-4}$
Tb^+	3.0	16.9	0.18	$TbCl^+$	100	$TbCl_2^+$, $TbCl_{1,2}^+(CH_3Cl)_{1-4}$
Dy^+	0.23	16.9	0.013	$DyCl^+$	~97	$DyCl_2^+$, $DyCl^+(CH_3Cl)_{1-3}$
				Dy^+CH_3Cl	~3	
Ho^+	0.16	16.9	9.5×10^{-3}	$HoCl^+$	~90	$HoCl_2^+$, $HoCl_{1,2}^+(CH_3Cl)_{1-4}$
				Ho^+CH_3Cl	~10	
Er^+	0.13	16.9	7.7×10^{-3}	$ErCl^+$	92	$ErCl_2^+$, $ErCl_2^+(CH_3Cl)$
				Er^+CH_3Cl	8	$Er^+(CH_3Cl)_{2,3}$
Tm^+	≤0.01	16.8	$\leq6.0\times10^{-4}$	$TmCl^+$	~70	—
				Tm^+CH_3Cl	~30	—
Yb^+	≤0.01	16.8	$\leq6.0\times10^{-4}$	$YbCl^+$	70	$YbCl^+(CH_3Cl)_{1,2}$
				Yb^+CH_3Cl	30	$Yb^+(CH_3Cl)_{2,3}$
Lu^+	1.2	16.7	0.072	$LuCl^+$	100	$LuCl_2^+$, $LuCl_2^+(CH_3Cl)_{1-4}$

Note: Products and product distributions are also included along with calculated collision rate coefficients (k_c, in 10^{-10} cm^3 molecule^{-1} s^{-1}, see text) and reaction efficiencies (k/k_c).

[a] Measured reaction rate coefficient with an estimated accuracy of ±30%.

[b] Calculated capture rate coefficient (see text).

[c] PD = product distribution expressed as a percentage.

uct ions that were observed. The higher order chemistry initiated by La^+, Gd^+, Dy^+, and Lu^+ can be tracked in Fig. 1.

Periodicities in reaction efficiencies

The primary CH_3Cl reaction efficiencies of the 14 Ln^+ cations change dramatically along the 4f row. The efficiencies of the reactions of La^+ (0.62), Ce^+ (0.55), and Gd^+ (0.59) are all higher than 0.50, and it is interesting to note that these cations all have two non-f electrons in their electronic ground state. In contrast, the efficiencies of the reactions of the early lanthanide cations Sm^+ (0.064) and Eu^+ (0.019) are ≤0.1 and those of the late lanthanide cations Dy^+ (0.013), Ho^+ (9.5×10^{-3}), Er^+ (7.7×10^{-3}), Tm^+ ($\leq 6.0 \times 10^{-4}$), and Yb^+ ($\leq 6.0 \times 10^{-4}$) are all <0.02, near or below the detection limit. An overview of the variation in reaction efficiency across the lanthanide series is included in Fig. 2.

Thermodynamics of Cl atom abstraction

Cl atom abstraction was observed with all the lanthanide cations. Rate coefficients measured for Cl atom abstraction are in the range $\leq 1.0 \times 10^{-12}$ cm^3 molecule^{-1} s^{-1} (for Tm^+ and Yb^+) to 1.1×10^{-9} cm^3 molecule^{-1} s^{-1} (for La^+). Assuming that only exothermic or thermoneutral reaction can be observed under our experimental operating conditions, we estimate that the chlorine atom affinity ($ClA(Ln^+)$) is higher than $ClA(CH_3)$ = 83.7 kcal mol^{-1} (19) for all the lanthanide cations investigated. Unfortunately, no Cl atom affinities appear to be available for any lanthanide cations, either from theory or from experiment. The lower limit of 83.7 kcal mol^{-1} for the 14 lanthanide cations investigated therefore represents the first such determination.

Mechanism for Cl atom abstraction by Ln^+

Two mechanisms have been proposed for the reactions of lanthanide cations with fluorinated hydrocarbons (22): a harpoonlike abstraction and C—F bond insertion. The first mechanism involves the transfer of an electron within the encounter complex $LnFR^+$, perhaps at long range, from the lanthanide cation to the fluorinated substrate. This favors the homolytic cleavage of the C—F bond to form LnF^+ according to rxn. [4]. The reaction efficiency predicted by this mechanism should correlate with the second ionization energy of Ln ($IE(Ln^+)$) as has been proposed by Cornehl et al. (22) in their attempt to account for their measured reaction rates with fluoromethane, 1,1-difluoroethane, fluorobenzene, and hexafluorobenzene.

$$[4] \quad Ln^+ + R\text{-}F \rightarrow [Ln^+\cdots F\text{-}R \rightarrow Ln^{2+}\text{-}F^-\cdots R] \rightarrow LnF^+ + R$$

In the C—F bond insertion mechanism, a cyclic ion complex is initially formed, which is then transformed through a three-centre transition state into a complex in which Ln^+ is

Table 2. Ln^+ ground-state valence configurations, term symbols, the promotion energies to first $5d^16s^1$ configuration, and the ionization energies of Ln^+.

Ln^+ species	Ln^+ ground-state valence configuration	Ln^+ term symbol[a]	Promotion energy to first $5d^16s^1$ configuration[a] (kcal mol^{-1})	IE Ln^{+}[b] (eV)
La^+	$5d^2$	$^3F_2$	4.5±3.0	11.06
Ce^+	$4f^15d^2$	$^4H_{7/2}{}^{o}$	4.6±5.7	10.85
Pr^+	$4f^36s^1$	$(9/2,1/2)_4{}^{o}$	22.3±0.8	10.55
Nd^+	$4f^46s^1$	$^6I_{7/2}$	34.8±8.3	10.72
Pm^+	$4f^56s^1$	$^7H_2{}^{o}$	46.4±7.2	11.07
Sm^+	$4f^66s^1$	$^8F_{1/2}$	62.1±5.8	11.07
Eu^+	$4f^76s^1$	$^9S_4{}^{o}$	92.8±5.0	11.25
Gd^+	$4f^75d^16s^1$	$^{10}D_{5/2}{}^{o}$	0.0	12.10
Tb^+	$4f^96s^1$	$(15/2,1/2)_8{}^{o}$	9.3±8.1	11.52
Dy^+	$4f^{10}6s^1$	$(8,1/2)_{17/2}$	36.0±6.1	11.67
Ho^+	$4f^{11}6s^1$	$(15/2,1/2)_8{}^{o}$	37.8±5.4	11.80
Er^+	$4f^{12}6s^1$	$(6,1/2)_{13/2}$	34.5±3.1	11.93
Tm^+	$4f^{13}6s^1$	$(7/2,1/2)_4{}^{o}$	55.5±7.4	12.05
Yb^+	$4f^{14}6s^1$	$^2S_{1/2}$	79.4±4.0	12.17
Lu^+	$4f^{14}6s^2$	$^1S_0$	36.6±3.6	13.90

[a] See ref. 24.
[b] See ref. 25.

Fig. 2. Reaction efficiency (closed circle for CH_3Cl and left ordinate axis) and the energy required to promote an electron and leave the Ln^+ cation in a d^1s^1 configuration (solid square and right ordinate axis) plotted along the lanthanide row of elements. There is an apparent correlation between reaction efficiency and electron promotion energy.

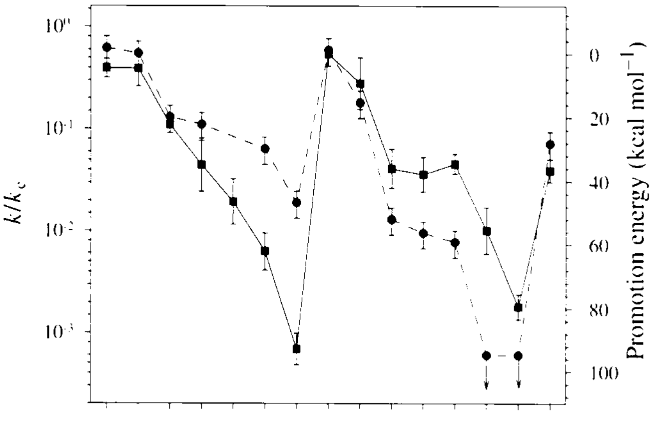

inserted into the R—F bond. The inserted complex can then eliminate the LnF^+ and R species. This mechanism requires that at least two Ln^+ electrons reside in non-f valence orbitals. The reaction efficiency predicted by this mechanism should correlate with the $4f^n6s^1$ to $4f^{n-1}5d^16s^1$ promotion energy (E_p). Our previous measurements of reactions of lanthanide cations with CH_3F provide reactivity correlations that demonstrate a preference for the C—F bond insertion mechanism, which also has been shown to apply to hydrocarbon activation by Ln^+ (1).

The experimental results reported here clearly show that the ability of Ln^+ to abstract a chlorine atom from methyl chloride does not correlate well with the second IE of the lanthanide (see Table 2 and Fig. 3). So we cannot assign a harpoonlike Cl abstraction mechanism to these reactions with CH_3Cl on the basis of such a correlation.

Our experimental results indicate that La^+ ($5d^2$) with two non-f valence electrons exhibits the highest efficiency for Cl atom abstraction followed closely by Gd^+ ($4f^75d^16s^1$) and Ce^+ ($4f^15d^2$) all of which also have two non-f valence electrons. The reactivities of the remaining Ln^+ cations (except Lu^+), all of which have available only one non-f electron (s^1), are all less and decrease along the early and late lanthanide series. So apparently the s electron at most plays a small role in determining these reactivities. Indeed, as shown in Figs. 2 and 4, these decreasing reactivities correlate well with the variation in the electron-promotion energy of Ln^+ required to achieve a $4f^{n-1}5d^16s^1$ configuration. Thus, f to d electron promotion appears crucial for the efficient occurrence of Cl atom transfer. This correlation indicates that two non-f electrons are required for Cl atom abstraction from CH_3Cl and that the reaction occurs via a C—Cl bond insertion mechanism. We note that the trend exhibited in Fig. 4 is remarkably similar to that presented by Cornehl et al. (23) for reactions of Ln^+ cations with saturated and unsaturated hydrocarbons and to that we have reported for reactions of Ln^+ with methyl fluoride (15) for which a C—X (X = C, H, or F) bond insertion mechanism also has been advanced. The small amounts of $Ln^+(CH_3Cl)$ adduct ions observed with the late lanthanide cations may be collisionally stabilized remnants of the inserted reaction intermediate. It is interesting to see that Lu^+, although having two electrons in non-f orbitals ($4f^{14}6s^2$), has a much lower reaction efficiency compared with La^+, Ce^+, and Gd^+; this can be attributed to the closed 6s and 4f subshells of Lu^+.

Inspection of our results for the addition of another Cl atom to $LnCl^+$ in a second reaction with CH_3Cl indicates that the second Cl atom transfers are fast (k > 1.4 × 10^{-10} cm^3 molecule^{-1} s^{-1}) with those Ln^+ cations with low

Fig. 3. The dependence of the efficiencies for Cl atom abstraction in reactions of Ln^+ with CH_3Cl on the second ionization energy of Ln (IE(Ln^+)).

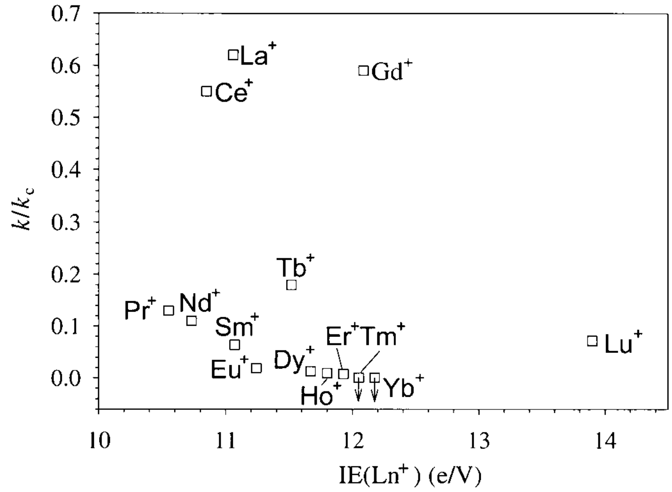

Fig. 4. Correlation of reaction efficiency for Cl atom abstraction from CH_3Cl with the energy E_p required to promote an electron and leave the Ln^+ cation in a d^1s^1 configuration. The dashed curve represents a fit with $k/k_c = 0.0081 + 0.66\ \exp(-0.078E_p)$.

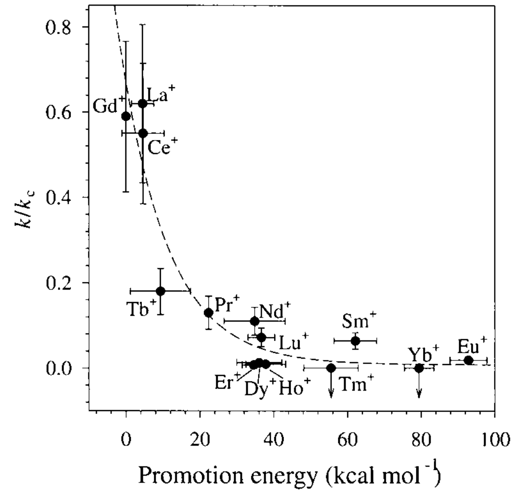

Fig. 5. Correlation of reaction efficiency with the electron promotion energy that is proposed to be required for Ln^{2+}—Cl^- bond formation in the reactions of early and late Ln^+ ions with CH_3Cl. Lu^+ clearly is an exception to the trend observed for the late Ln^+ ions. The slopes of these van't Hoff-like plots provide characteristic temperatures of $(1.4 \pm 0.2) \times 10^4$ and $(4.5 \pm 0.3) \times 10^3$ K for Cl atom abstraction with the early and late lanthanide cations, respectively.

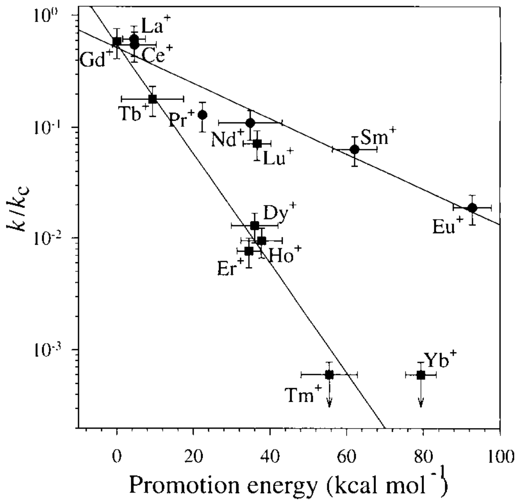

promotion energies ($E_p < 9.3$ kcal mol^{-1}) and slow ($k < 5.4 \times 10^{-11}$ cm^3 $molecule^{-1}$ s^{-1}) with those Ln^+ cations with high promotion energies ($E_p > 92.8$ kcal mol^{-1}). Such a reactivity pattern again is not inconsistent with an insertion mechanism that requires two unpaired valence electrons.

Arrhenius-like plots

Figure 5 demonstrates, in an Arrhenius-like plot, that the reaction efficiency of the Ln^+ reactions with CH_3Cl, here measured at constant temperature (295 K), exhibits an exponential dependence on the promotion energy according to eq. [5].

$$[5] \quad k/k_c = \exp(-XE_p)$$

A remarkable aspect of these results is the distinct difference in this dependence between the early and late lanthanide ions. If interpreted as $1/RT_{\text{eff}}$, the slopes of the semilogarithmic plots in Fig. 5 indicate "characteristic temperatures" of $(1.4 \pm 0.2) \times 10^4$ and $(4.5 \pm 0.3) \times 10^3$ K for Cl atom abstraction with the early and late lanthanide cations, respectively. The indicated accuracy is the standard error derived from the fit. The exact physical meaning of these characteristic temperatures is not completely clear, but we postulate, as we have done before for reactions of Ln^+ with CH_3F (15), that the difference in characteristic temperature can be attributed to an energy associated with the electron promotion. Electron promotion in the early lanthanide ions involves an unpaired f electron while that in the late lanthanide ions involves a paired f electron. Thus, electron promotion in the late lanthanide ions involves electron–electron repulsion and so can be expected to be more effective and exhibit a lower characteristic temperature. It is noteworthy that the characteristic temperatures obtained for the Cl atom abstraction from CH_3Cl with the early and late lanthanide cations are similar to those for F atom abstraction from CH_3F, $(1.80 \pm 0.24) \times 10^4$ and $(4.4 \pm 0.2) \times 10^3$ K, respectively (15). This would be expected since F atom abstraction from CH_3F also requires the electronic excitation of Ln^+ by electron promotion (15).

Comparison of the reactivities of lanthanide cations towards CH_3Cl and CH_3F

A comparison of the reactivities that we have measured previously with CH_3F (15) shows that all the lanthanide cations, except for Lu^+, react more efficiently with CH_3Cl than with CH_3F; Fig. 6 indicates that values for $k/k_c(CH_3Cl)/k/k_c(CH_3F)$ range from 1.0 (for Eu^+) to 3.4 (for Dy^+). This can be attributed to at least two causes. The Cl—CH_3 bond is much weaker than the F—CH_3 bond (the bond dissociation energies for Cl—CH_3 and F—CH_3 are 83.7 and 112.9 kcal mol^{-1}, respectively (19)), and this makes

Fig. 6. Comparison of the reaction efficiencies of the reactions of Ln^+ with CH_3F and CH_3Cl.

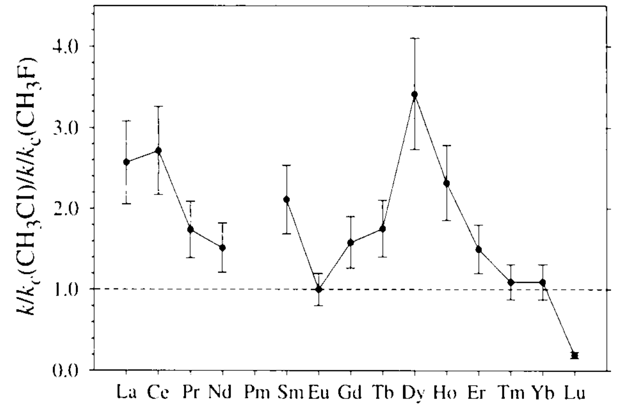

the Cl abstraction more exothermic than the F atom abstraction, which reduces the kinetic barrier. Also, the electrostatic interaction between Ln^+ and CH_3Cl is stronger than that between Ln^+ and CH_3F since CH_3Cl has a much higher polarizability (4.72×10^{-24} cm^3 compared with 2.97×10^{-24} cm^3 for CH_3F (19)) and a slightly higher dipole moment (1.896 D vs. 1.858 D (19)), and this also lowers the kinetic barrier with respect to the initial energy of the reactants.

The T_{eff} (($4.5 \pm 0.3) \times 10^3$ K) for the reactions of the late lanthanide cations with CH_3Cl obtained in Fig. 5 is close to the value for CH_3F (($4.4 \pm 0.2) \times 10^3$ K) (15), while the T_{eff} (($1.4 \pm 0.2) \times 10^4$ K) for the reactions of the early lanthanide cations with CH_3Cl is close to, but distinctly below, the value for CH_3F (($1.80 \pm 0.24) \times 10^4$ K) (15). This may imply that stronger carbon–halogen bonds result in higher values for T_{eff}, but the effect on the reaction efficiency for the late lanthanide cations is much weaker than that for the early lanthanide cations.

We have previously found (15) that Lu^+ is quite reactive with CH_3F ($k/k_c = 0.37$) even though it has a $4f^{14}6s^2$ ground electronic configuration and a high s to d promotion energy (36.6 kcal mol^{-1}). We suggested that this apparent anomaly might be explained by the overlap of the $6s^2$ orbital with the antibonding orbital of methyl fluoride. This will weaken the F—CH_3 bond sufficiently to enable F atom transfer without the need for s to d promotion. In this work, Lu^+ was found to be much less reactive towards CH_3Cl ($k/k_c = 0.072$) compared with CH_3F. This may imply that the orbital levels of $6s^2$ of Lu^+ and the antibonding orbital of CH_3Cl do not match for overlapping so that the promotion energy governs the reactivity in this case.

Conclusions

Lanthanide cations have been observed to react with methyl chloride at room temperature predominantly by Cl atom transfer. The efficiency of this transfer correlates with the energy required to promote an electron to achieve a d^1s^1 excited electronic configuration in which two non-f electrons are available for bonding. The efficiency decreases as the promotion energy increases and the periodic trend in reaction efficiency along the lanthanide series matches the periodic trend in the corresponding electron promotion energy. This behavior is consistent with a C—Cl bond insertion mechanism of the type previously proposed for C—F, C—H, and C—C bond activation reactions of Ln^+ cations with alkanes and alkenes (23). Direct Cl atom abstraction by a harpoonlike mechanism can be excluded on the basis of an observed noncorrelation of reaction efficiency with IE(Ln^+). A remarkable Arrhenius-like correlation is observed for the dependence of reactivity on promotion energy: the early and late lanthanide cations exhibit characteristic temperatures of ($1.4 \pm 0.2) \times 10^4$ and ($4.5 \pm 0.3) \times 10^3$ K, respectively. A rapid, second Cl atom transfer occurs with $LaCl^+$, $CeCl^+$, $GdCl^+$, $TbCl^+$, and $LuCl^+$, but there was no evidence for a third chlorine atom abstraction with any of the $LnCl_2^+$ cations. Both $LnCl^+$ and $LnCL_2^+$ can sequentially add up to five methyl chloride molecules under the experimental operating conditions of the ICP/SIFT tandem mass spectrometer.

Acknowledgments

Continued financial support from the Natural Sciences and Engineering Research Council of Canada (NSERC) is greatly appreciated. Also, we acknowledge support from the National Research Council of Canada, the Natural Sciences and Engineering Research Council, and MDS SCIEX in the form of a Research Partnership grant. As holder of a Canada Research Chair in Physical Chemistry, Diethard K. Bohme acknowledges the contributions of the Canada Research Chair Program to this research.

References

1. J.B. Schilling and J.L. Beauchamp. J. Am. Chem. Soc. **110**, 15 (1988).
2. D.K. Bohme. The encyclopedia of mass spectrometry. Vol. 4. Elsevier Ltd., London, UK. 2005. pp. 638–648.
3. J.L. Elkind, L.S. Sunderlin, and P.B. Armentrout. J. Phys. Chem. **93**, 3151 (1989).
4. G.K. Koyanagi and D.K. Bohme. J. Phys. Chem. A, **105**, 8964 (2001).
5. Y. Huang, M.B. Wise, D.B. Jacobson, and B.S. Freiser. Organometallics, **6**, 346 (1987).
6. J.K. Gibson. J. Phys. Chem. **100**, 15688 (1996).
7. M. Azzaro, S. Breton, M. Decouzon, and S. Geribaldi. Int. J. Mass Spectrom. Ion Processes, **128**, 1 (1993).
8. S. Geribaldi, S. Breton, M. Decouzon, and M. Azzaro. J. Am. Soc. Mass. Spectrom. **7**, 1151 (1996).
9. J.M. Carretas, J. Marcalo, and A. Pires de Matos. Int. J. Mass Spectrom. **234**, 51 (2004).
10. J.K. Gibson and R.G. Haire. Radiochimica Acta, **89**, 709 (2001).
11. W.W. Yin, A.G. Marshall, J. Marcalo, and A. Pires de Matos. J. Am. Chem. Soc. **116**, 8666 (1994).
12. J.M. Carretas, A. Pires de Matos, J. Marcalo, M. Pissavini, M. Decouzon, and S. Geribaldi. J. Am. Soc. Mass. Spectrom. **9**, 1035 (1998).
13. N. Marchande, S. Breton, S. Geribaldi, J.M. Carretas, A. Pires De Matos, and J. Marcalo. Int. J. Mass Spectrom. **195/196**, 139 (2000).
14. M. da Conceicao Vieira, J. Marcalo, and A. Pires de Matos. J. Organomet. Chem. **632**, 126 (2001).
15. G.K. Koyanagi, X. Zhao, V. Blagojevic, M.J.Y. Jarvis, and D.K. Bohme. Int. J. Mass Spectrom. **241**, 189 (2005).

16. G.K. Koyanagi, V.V. Lavrov, V. Baranov, D. Bandura, S. Tanner, J.W. McLaren, and D.K. Bohme. Int. J. Mass Spectrom. **194**, L1 (2000).
17. G.K. Koyanagi, V.I. Baranov, S.D. Tanner, and D.K. Bohme. J. Anal. At. Spectrom. **15**, 1207 (2000).
18. T.C. Su and W. J. Chesnavich. J. Chem. Phys. **76**, 5183 (1982).
19. D.R. Lide (*Editor*). CRC handbook of chemistry and physics. 80th ed. CRC Press, Boca Raton, Florida. 2001.
20. K. Kimura, S. Katsumata, Y. Achiba, T. Yamazaki, and S. Iwata. *In* Handbook of HeI photoelectron spectra of fundamental organic compounds. Japan Scientific Soc. Press, Tokyo. 1981.
21. P.B. Armentrout. Int. J. Mass Spectrom. **227**, 289 (2003).
22. H.H. Cornehl, G. Hornung, and H. Schwarz. J. Am. Chem. Soc. **118**, 9960 (1996).
23. H.H. Cornehl, C. Heinemann, D. Schroder, and H. Schwarz. Organometallics, **14**, 992 (1995).
24. Z.B. Goldschmidt. Handbook on the physics and chemistry of rare earths. North-Holland Publishing Co, Amsterdam. 1978. p. 79.
25. C.E. Moore. Nat. Stand. Ref. Data Ser. Nat. Bur. Stand. **34**, 1 (1970).